

Timing, Position, Navigation, and Communications for Distributed Small Spacecraft Beyond Low Earth Orbit (LEO)

Abstract: CubeSat systems have the potential to make significant contributions to multiple areas of astrophysics research, including detection of gravitational wave counterparts, Gamma Ray Bursts (GRBs) and GRB afterglow, X-ray and ultraviolet astrophysics, exoplanet studies, solar, ionospheric and space physics, and variable star astrophysics including pulsar detection, Active Galactic Nuclei (AGN) physics, transient, time domain, and multi-messenger astrophysics. Several of these areas of astrophysical research utilize the radio frequency (RF) spectrum between 10 MHz and 10 GHz. This spectrum accounts for significant opportunities for research with space-based CubeSat systems and networks. While other frequency ranges such as millimeter-wave bands are important for research, the 10 MHz to 10 GHz frequency bands are optimum for CubeSat applications. Given this wide frequency range, the question becomes how to incorporate this capability in small form factor CubeSats. Swarms or constellations of CubeSats can be configured to perform multi-aperture Very Long Baseline Interferometry (VLBI), which is a fundamental technique for radio astronomy. These long apertures required for VLBI make it difficult, if not impossible, to synchronize the timing, position, navigation, and communications among the individual interferometer elements. Since the CubeSat interferometer will be operating in deep space at, for example, the second Lagrange Point (LP2) at a distance of 1.5 million kilometers, interface with near earth systems such as GPS will not be possible. One solution to this is to use nature's clocks, i.e., pulsars, to provide accurate timing signals which can be utilized in turn for position, navigation, and communications of the individual CubeSat elements as well as the entire interferometer array. Two types of pulsars can be utilized; one which emits an electromagnetic radio frequency or one that produces X-rays. While both techniques will be addressed, the electromagnetic radio frequency pulsar case will be discussed in detail.

1. Introduction

As introduced in Hinzl, D., 2024, TechRxiv [Application of CubeSats for Astrophysics Research: Detection of Radio Frequency Counterparts of High Energy Phenomena with Very Long Baseline Interferometry](#), TechRxiv, DOI: [10.36227/tech arxiv.172902594.41726347/v1](#), an interferometer operating at Lagrange Point LP2 will likely require a timing reference signal that is independent of near earth systems. Telescopes in a traditional ground based interferometer are connected via cables so that their signals can be combined in real time. For a CubeSat network, the individual CubeSat units can be phase synchronized for coherent operation across the entire array (or subarray) in several ways depending on where they are deployed. In a low earth orbit application, GPS can be the timing mechanism. Alternatively, a ground based timing and synchronizing network could be employed and signals uplinked to the array. For a deep space application such as around one of the LaGrange Points, one or more of the CubeSat units would have to take on the role as the timing source. Another option is the use of pulsars with the [International Pulsar Timing Array \(IPTA\)](#) which incorporates approximately 100 millisecond pulsars as a galactic system of highly accurate clocks. Each pulsar (a rapidly rotating neutron star) typically has a rotational period of less than 10 milliseconds with an accuracy of 100 nanoseconds. This study will explore the use of pulsars as the timing signal source and show how this can be utilized for spacecraft position, navigation and communications.

A [pulsar](#) is a highly magnetized rotating [neutron star](#) that emits beams of [electromagnetic radiation](#) out of its [magnetic poles](#). This radiation can be observed only when a beam of emission is pointing toward Earth (much like the way a lighthouse can be seen only when the light is pointed in the direction of an observer), and is responsible for the pulsed appearance of emission. Neutron stars are very [dense](#), and have short, regular rotational [periods](#). This produces a very precise interval between pulses that ranges from milliseconds to seconds for an individual pulsar. The periods of pulsars make them very useful tools for astronomers. Observations of a pulsar in a [binary neutron star system](#) were used to indirectly confirm the existence of [gravitational radiation](#). The first [extrasolar planets](#) were discovered around a pulsar, [PSR B1257+12](#). Certain types of pulsars rival [atomic clocks](#) in their accuracy in [keeping time](#). Figure A1 depicts pulsar geometry.

2. Background

As mentioned, the two techniques for spacecraft timing with pulsars are X-Ray pulsars and Radio Frequency (RF) pulsars.

2.1 X-Ray Pulsars

[X-Ray pulsars](#) or accretion-powered pulsars are sources exhibiting strict periodic variation in X-Ray intensity, within the range of a fraction of a second to years. An X-ray [pulsar](#) is a type of [binary star system](#) consisting of a typical star (stellar companion) in orbit around a magnetized [neutron star](#). The [magnetic field](#) strength at the surface of the neutron star is typically about 10^8 [Tesla](#), over a trillion times stronger than the strength of the magnetic field measured at the [surface of the Earth](#) ($60 \mu\text{T}$). There are two main classes of X-Ray binaries, Low Mass X-Ray Binaries (LMXBs) and High Mass X-Ray Binaries (HMXBs). LMXBs consist of a white dwarf and a dim main sequence M or K star orbiting in a binary pair, with the white dwarf accreting matter from the companion star. HMXBs consist of either a black hole or neutron star accreting matter from young, massive, bright O or B spectral type companion stars. [Stellar classification](#) is a classification of stars based on their spectral characteristics. Pulsar-based navigation and timing is a navigation technique whereby the periodic [X-ray](#) signals emitted from [pulsars](#) are used to determine the location of a vehicle, such as a spacecraft in deep space. A vehicle using X-ray pulsar-based navigation and timing would compare received X-ray signals with a database of known pulsar frequencies and locations. Similar to [GPS](#), this comparison would allow the vehicle to calculate its position accurately. The advantage of using X-ray signals over [radio waves](#) is that [X-ray telescopes](#) can be made smaller and lighter than radio frequency receivers.

2.2 Electromagnetic RF Pulsars

[Millisecond Pulsars](#) are pulsars with a rotational period less than about 10 milliseconds. Millisecond pulsars have been detected in radio, X-Ray, and gamma ray portions of the electromagnetic spectrum. The leading hypothesis for the origin of millisecond pulsars is that they are old, rapidly rotating [neutron stars](#) that have been spun up or "recycled" through [accretion](#) of matter from a companion star in a close binary system. Millisecond pulsars are thought to be related to [low-mass X-ray binary](#) systems. It is thought that the X-rays in these systems are emitted by the [accretion disk](#) of a [neutron star](#) produced by the outer layers of a companion star that has overflowed its [Roche lobe](#). The

transfer of [angular momentum](#) from this accretion event can increase the rotation rate of the pulsar to hundreds of times per second, as is observed in millisecond pulsars.

Many millisecond pulsars are found in [globular clusters](#). This is consistent with the spin-up hypothesis of their formation, as the extremely high stellar density of these clusters implies a much higher likelihood of a pulsar having (or capturing) a giant companion star. Currently there are approximately 130 millisecond pulsars known in globular clusters. The globular cluster [Terzan 5](#) contains 37 of these, followed by [47 Tucanae](#) with 22 and [M28](#) and [M15](#) with 8 pulsars each. The first millisecond pulsar, [PSR B1937+21](#), was discovered in 1982. Spinning roughly 641 times per second, it remains the second fastest-spinning millisecond pulsar of the approximately 200 that have been discovered. Pulsar [PSR J1748-2446ad](#), discovered in 2004, is the fastest-spinning pulsar known, as of 2023, spinning 716 times per second. Millisecond pulsars, which can be timed with high precision, have a stability comparable to [atomic-clock](#)-based time standards when averaged over decades. This also makes them very sensitive probes of their environments. For example, anything placed in orbit around them causes periodic [Doppler shifts](#) in their pulses' arrival times on Earth, which can then be analyzed to reveal the presence of the companion and, with enough data, provide precise measurements of the orbit and the object's mass. The technique is so sensitive that even objects as small as asteroids can be detected if they happen to orbit a millisecond pulsar. The first confirmed [exoplanets](#), discovered several years before the first detections of exoplanets around "normal" solar-like stars, were found in orbit around a millisecond pulsar, [PSR B1257+12](#). There are several pulsar catalogs and databases. These include:

- [The ATNF Pulsar Catalogue](#)
- [Jodrell Bank Pulsar Group](#)
- [National Radio Astronomy Observatory \(NRAO\)](#)

3. Methods and Concept of Operations

3.1 System Orbital Geometry

As introduced in Hinzl, D., 2024, TechRxiv [Application of CubeSats for Astrophysics Research: Detection of Radio Frequency Counterparts of High Energy Phenomena with Very Long Baseline Interferometry](#), TechRxiv, DOI: [10.36227/tech arxiv.172902594.41726347/v1](#), an interferometer operating at Lagrange Point LP2 will likely require a timing reference signal that is independent of near earth systems. This will require a very accurate determination of the location of electromagnetic radio frequency pulsars. Figure 1 and Figure 2 illustrate the geometry of Lagrange Point LP2 relative to the Sun, Moon, and Earth orbital configuration.

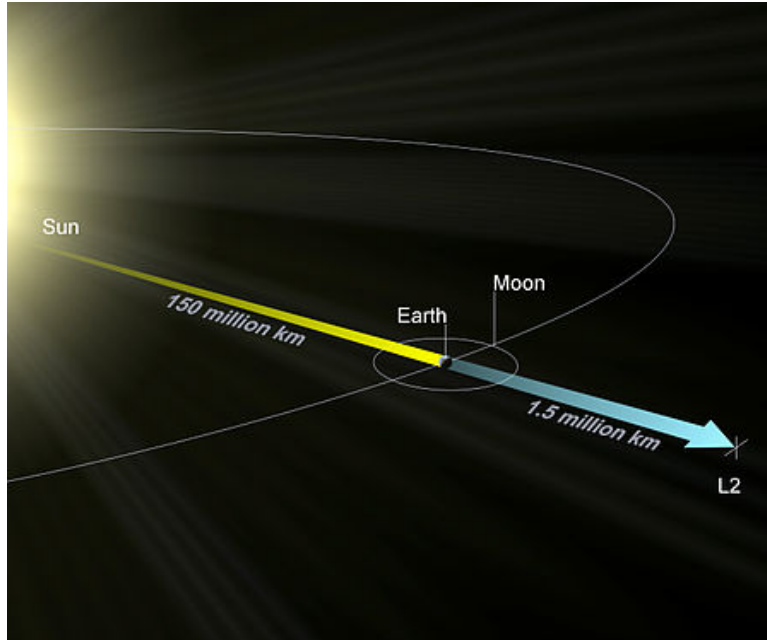


Figure 1. Lagrange Point LP2 in-plane view (Courtesy Wikipedia)

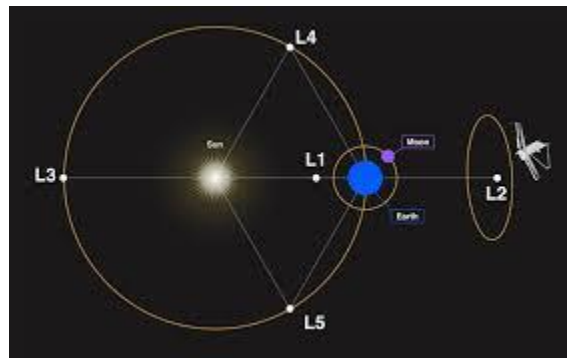


Figure 2. Lagrange Point LP2 overhead view (Courtesy Wikipedia)

From this orbital geometry and for a given location of the CubeSat (LP2), pulsars used for timing, position, navigation, and communications can be located with the coordinate system illustrated in Figures 3 and 4. Figure 3 shows the local CubeSat geometry at LP2 and Figure 4 shows the barycentric geometry of three reference pulsars for CubeSat positioning. In Figure 3, the CubeSat measures the angular position of a target pulsar in the form of a right ascension and declination pair (a,d) as follows:

$$a = a(i) \tan^{-1} \left[\frac{y - y(i)}{x - x(i)} \right] + e(1)$$

$$d = a(i) \tan^{-1} \left[\frac{z - z(i)}{\sqrt{[x - x(i)]^2 + [y - y(i)]^2}} \right] + e(2)$$

Here, $[x(i), y(i), z(i)]$ is the [Earth Centered Coordinates](#) position of the i th pulsar and $e = [e(1), e(2)]$ is the measurement noise.

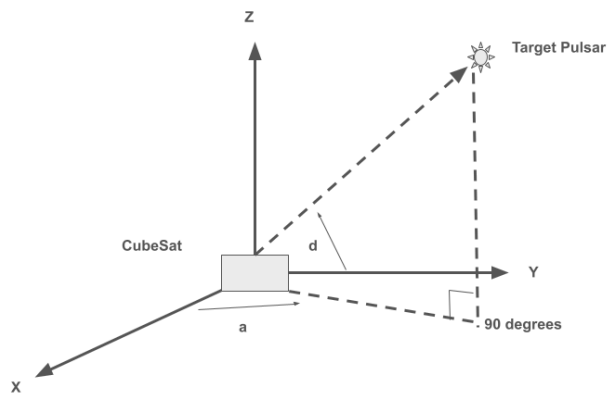


Figure 3. CubeSat Geometry

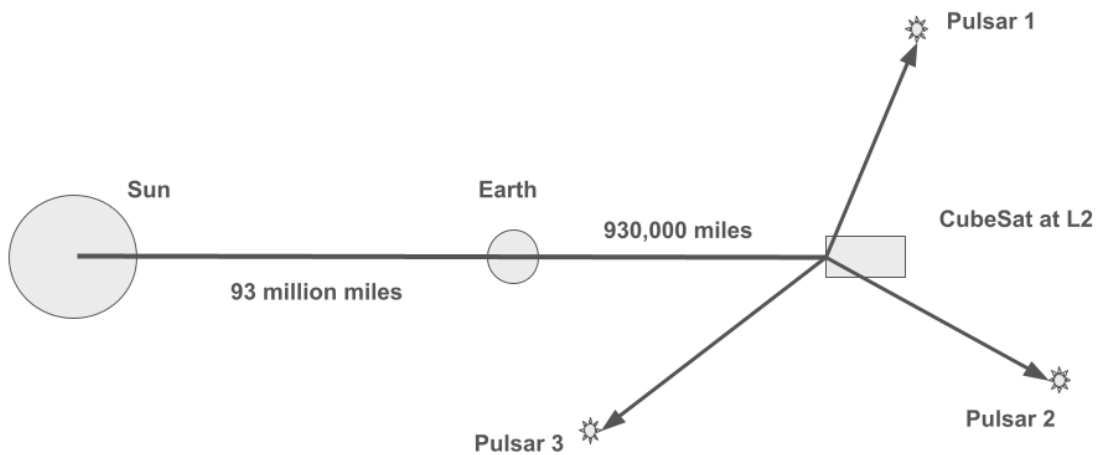


Figure 4. CubeSat Geometry (Three Pulsar Coordinates)

Here, Pulsar 1 (target pulsar) is J1300+1240.

Target Pulsar: J1300+1240

JNAME: J1300+1240 (JName: Pulsar name based on J2000 coordinates)

RAJ: 13:00:03.5767 (RAJ: Right ascension (J2000) (hh:mm:ss.s))

DECJ: +12:40:56.4721 (DecJ: Declination (J2000) (+dd:mm:ss))

P0: 0.00621853194840048 (P0: Barycentric period of the pulsar (s))

F0: 160.8096586618355 (F0: Barycentric rotation frequency (Hz))

DM: 10.16550 (Dispersion measure (cm-3 pc))

J1300+1240 is shown in Figures 5 and 6 for photometric pattern matching and optical field of view, respectively.

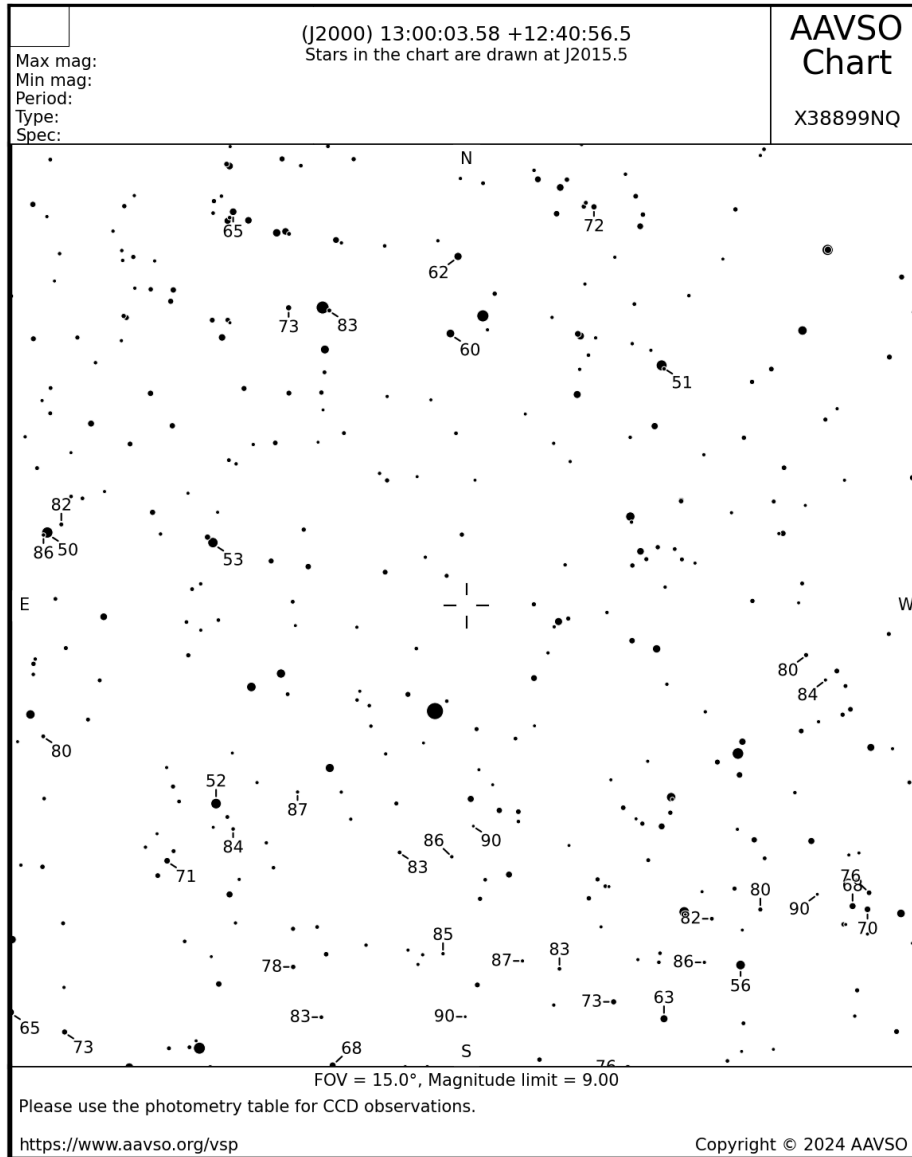


**Figure 5: Pulsar J1300+1240 Photometry Pattern Matching
(Courtesy American Association of Variable Star Observers)**

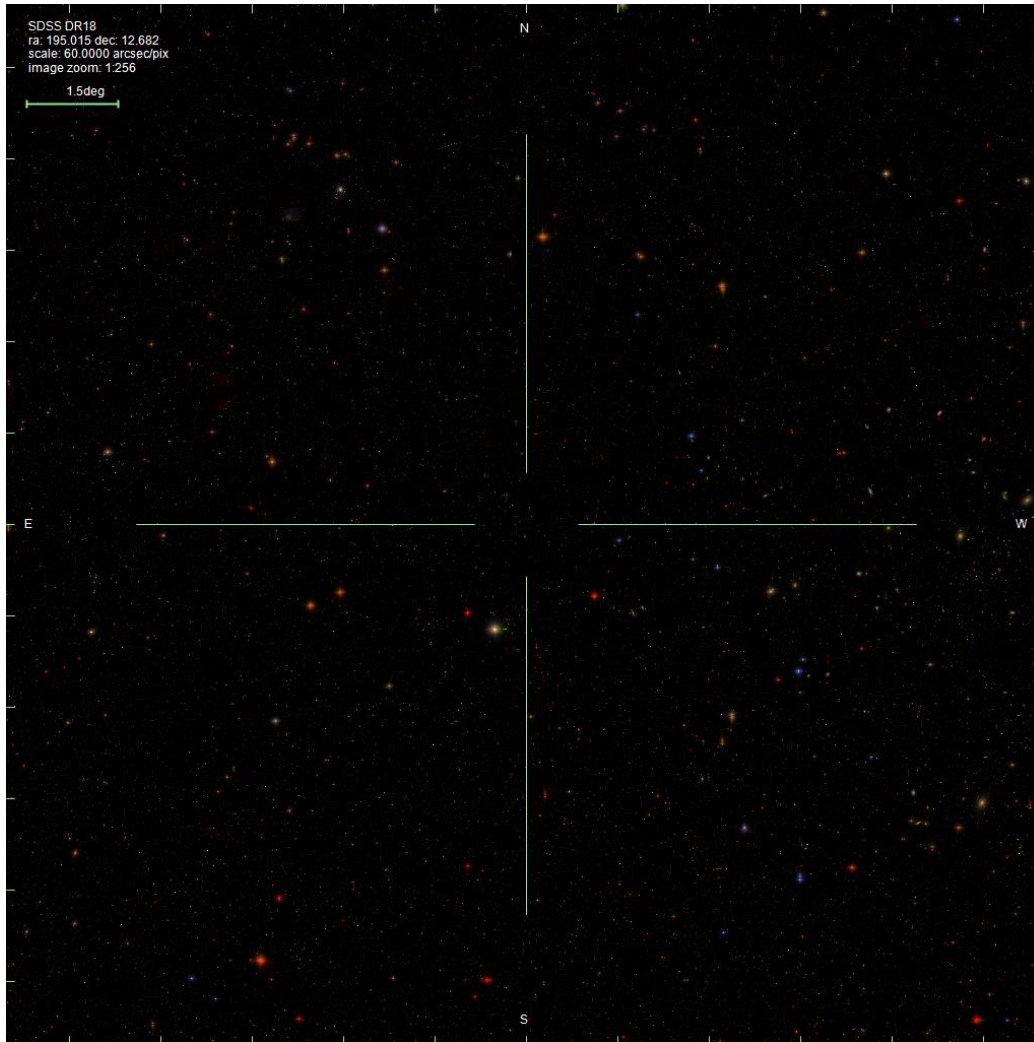


**Figure 6: Pulsar J1300+1240 Optical Field of View
(Courtesy Sloan Digital Sky Survey (SDSS) Data Release 18)**

Pulsars 2 and 3 have parameters as follows:

RAJ: 00:02:58.17

DECJ: +62:16:09.4

P0: 0.1153635682680

F0: 8.66824782740

DM:10

RAJ: 00:06:04.8

DECJ: +18:34:59

P0: 0.693748

F0: 1.441446

DM: 11.41

Taking pulsar J1300+1240 as an example, the pulsar coordinates are measured in [Barycentric Coordinate System](#) coordinates. The [barycenter](#) is the center of mass of two or more bodies that orbit one another and is the point about which the bodies orbit. A barycenter is a dynamical point, not a physical object. The distance from a body's center of mass to the barycenter can be calculated as a [two-body problem](#). If one of the two orbiting bodies is much more massive than the other and the bodies are relatively close to one another, the barycenter will typically be located within the more massive object. In this case, rather than the two bodies appearing to orbit a point between them, the less massive body will appear to orbit about the more massive body, while the more massive body might be observed to wobble slightly. This is the case for the Earth–Moon system, whose barycenter is located on average 4,671 km (2,902 mi) from Earth's center, which is 74% of Earth's radius of 6,378 km (3,963 mi). When the two bodies are of similar masses, the barycenter will generally be located between them and both bodies will orbit around it. When the less massive object is far away, the barycenter can be located outside the more massive object. This is the case for the system illustrated in Figures 1, 2, and 4 above with the barycenter slightly outside the Sun due to the relatively large distances involved.

Barycentric coordinates are non-rotating coordinates with the origin at the barycenter of two or more bodies. The [International Celestial Reference System \(ICRS\)](#) is a barycentric coordinate system centered on the Solar System's barycenter. Therefore, the CubeSat position can be determined within the barycenter coordinate system, since all objects (Sun, Earth, and CubeSat) lie in the same plane. Given the known position of the CubeSat, the angular geometry between the CubeSat and the pulsar can be determined in the form of a right ascension and declination pair (a, d) as shown in Figure 3. Similarly, optical stars can be used to determine the location and attitude of the CubeSat. This is depicted in Figures 5 and 6 which show the relative positions of optical stars and the target pulsar. Figure 5 includes numbered stars that are used for comparison and check stars for optical photometry and can be used for highly accurate position determination of the CubeSat.

Given the orbital geometry of the CubeSat system, the right ascension and declination pair (a, d) of Figure 3 can be translated back to [Earth Centered Coordinates](#) so that the location of all bodies (CubeSat, Sun, stars, etc.) can be accurately known in terms of Earth coordinates. A sun sensor on the CubeSat will accurately determine the position of the Sun at all times relative to the other bodies in the orbital system. From here, the pulsar signals can be used for highly accurate CubeSat timing applications. Upon detection of the radio frequency counterpart of a high energy astrophysical event, the relevant data will be downlinked to the ground station as described in Hinzel, D., 2024, TechRxiv.

About 3300 pulsars are known. Almost all of these are located within the Milky Way Galaxy, most within the galactic disk. About half of the 90 known millisecond pulsars (MSPs) are found in globular clusters; the high concentrations of stars in the cores of these clusters facilitate the recycling of old neutron stars to millisecond periods. The Galactic distribution of the Milky Way pulsars, including pulsars found in the Magellanic Clouds, is shown in Figure A2. Most of the pulsars reside in the Galactic plane, but a number are located at higher Galactic latitudes. Different sub-populations are shown. Figure A3 shows the ATNF Pulsar Catalog and the parameters utilized within the catalog.

3.2 Pulsar Timing

For the above example of pulsar J1300+1240, the radio frequency pulse is P0: 0.00621853194840048 (P0: Barycentric period of the pulsar (s)) and F0: 160.8096586618355 (F0: barycentric rotation frequency (Hz)). These numbers are reciprocals of each other. In terms of radar-type signals, P0 would be the radar's Pulse Repetition Interval (PRI) and F0 would be the radar's Pulse Repetition Frequency (PRF). As a further example, [LOFAR Discovery of a 23.5 s Radio Pulsar](#); C. M. Tan *et al* 2018 *ApJ* 866 54, DOI 10.3847/1538-4357/aade88, presents in great detail the measurement of a typical radio pulsar that can be utilized for CubeSat timing and other functions. In particular, Figure 7 denotes the relevant pulsar parameters important in CubeSat timing. Figure 8 shows typical pulsar pulses at 129 MHz, 168 MHz, and 350 MHz. Other frequencies discussed in Tan, et al. are 117.7, 133.3, 148.9, 164.6, 180.2, 1484, and 1532 MHz. From this it can be seen that pulsar timing pulses can be obtained at a variety of frequencies.

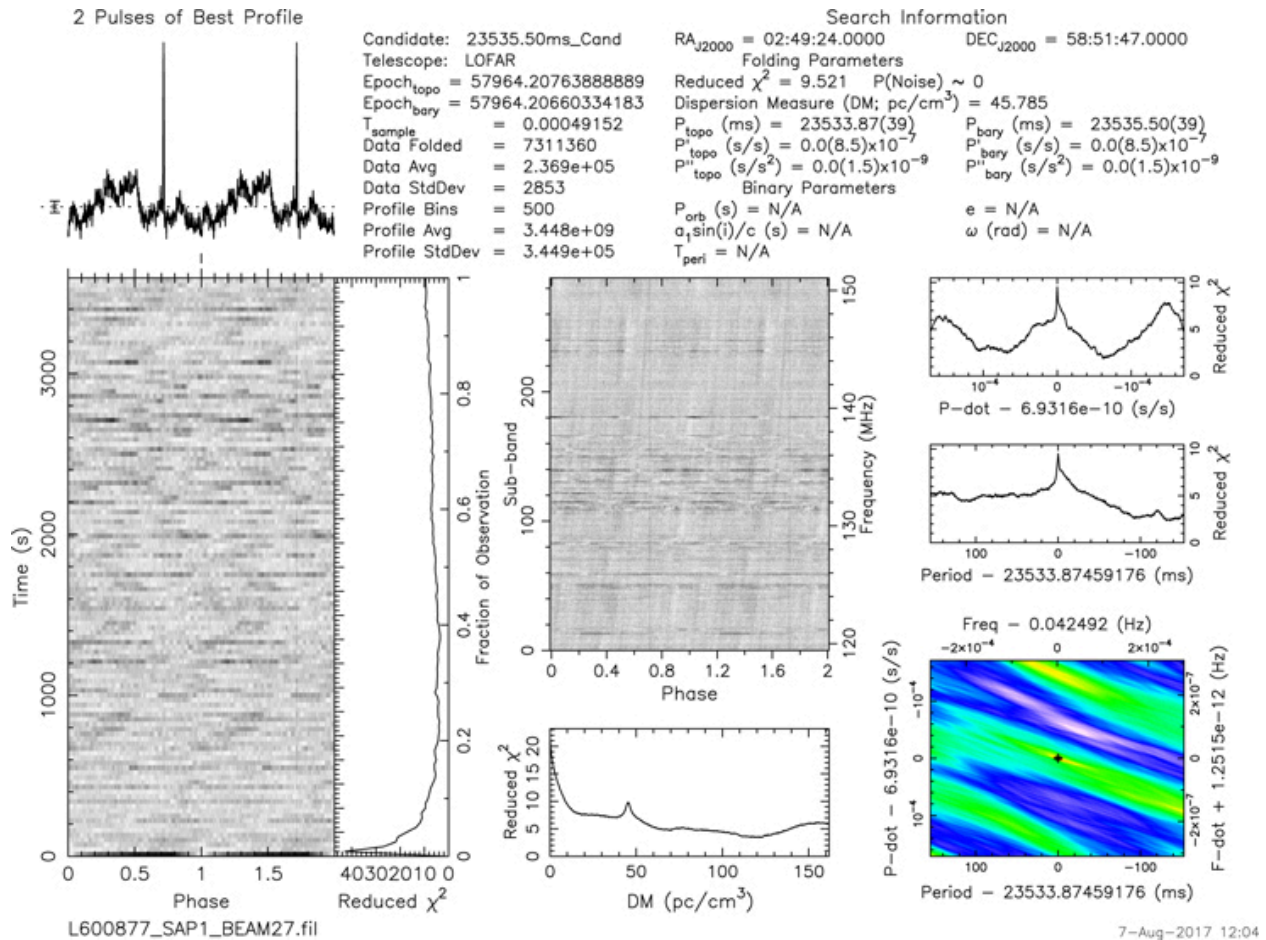


Figure 7: Pulsar PSR J0250+5845 with Fundamental Period of 23.535 Seconds
 (Figure 1 of C. M. Tan *et al*)

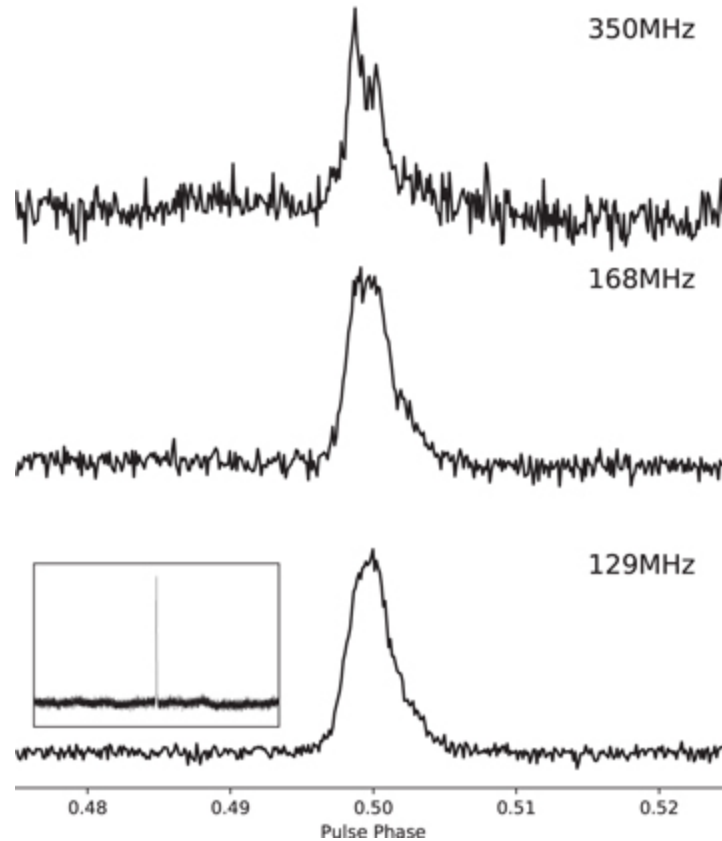


Figure 8: Pulsar PSR J0250+5845 Integrated Pulse Profile at Three Different Frequencies (Figure 6 of C. M. Tan *et al*)

Figures 7 and 8 above have been generated by [PRESTO: Pulsar Exploration and Search Toolkit](#). PRESTO is a large suite of pulsar search and analysis software. It was primarily designed to efficiently search for binary millisecond pulsars from long observations of globular clusters. To date, PRESTO has discovered well over a hundred and fifty pulsars, including approximately 100 recycled pulsars, about 80 of which are in binaries. It is written primarily in ANSI C, with many of the recent routines in Python.

4. Detailed Design

Figures 9 and 10 present the detailed design of the [Ettus](#) USRP N310 receiver as discussed in [Application of CubeSats for Astrophysics Research: Detection of Radio Frequency Counterparts of High Energy Phenomena with Very Long Baseline Interferometry](#), TechRxiv, DOI: [10.36227/techrxiv.172902594.41726347/v1](#), Hinzl, D., 2024, TechRxiv. The N310 utilizes a PPS (Pulse Per Second) signal for timestamp synchronization as seen in Figure 9. The PPS requires a square wave signal with 5 Vpp (Volts peak to peak) amplitude. The 23.5 second pulsar pulse can be used to create the required PPS signal, but will likely require a timing circuit that converts the pulsar signal to the PPS signal. This can be achieved in several ways, including a hardware pulse generator, a microcontroller with appropriate software, or an FPGA (Field Programmable Gate Array) with custom software.

Figure 11 shows the design of a pulsar timing method. The antennas utilized for pulsar timing functions are similar to those discussed in Hinzl, D., 2024, TechRxiv. Specifically, for the frequencies outlined above (117.7 MHz-1532 MHz), the antennas utilized are Midband 1: 550 MHz-2.0 GHz and Midband 2: 130 MHz-550 MHz. These are Figures A22-A26 and Figures A27-A29, respectively. The filters for each band are tunable MEMS bandpass filters. Direct RF sampling (RF to digital with an Analog-to-Digital Converter) is used rather than a heterodyne approach, and an FPGA generates the PPS and reference signals (and possibly other signals) to the N310 receiver.

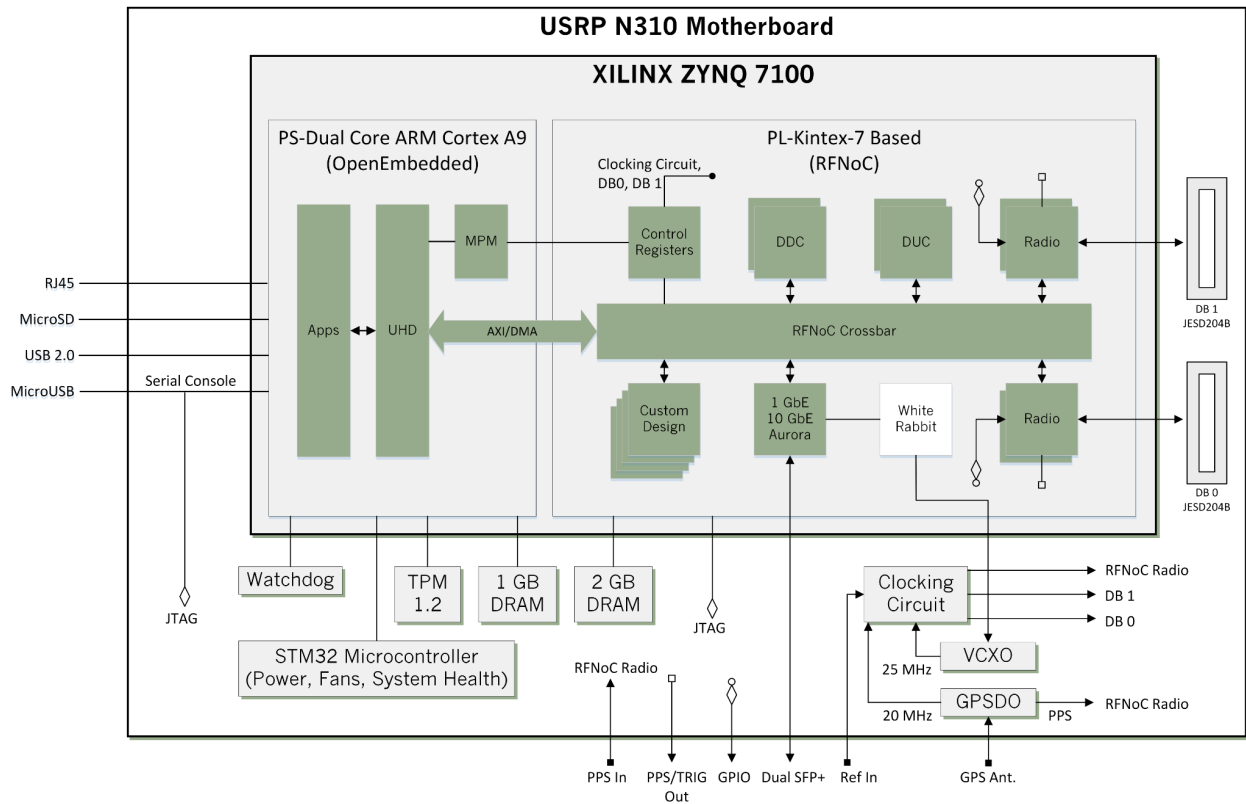


Figure 9: Ettus USRP N310 Motherboard

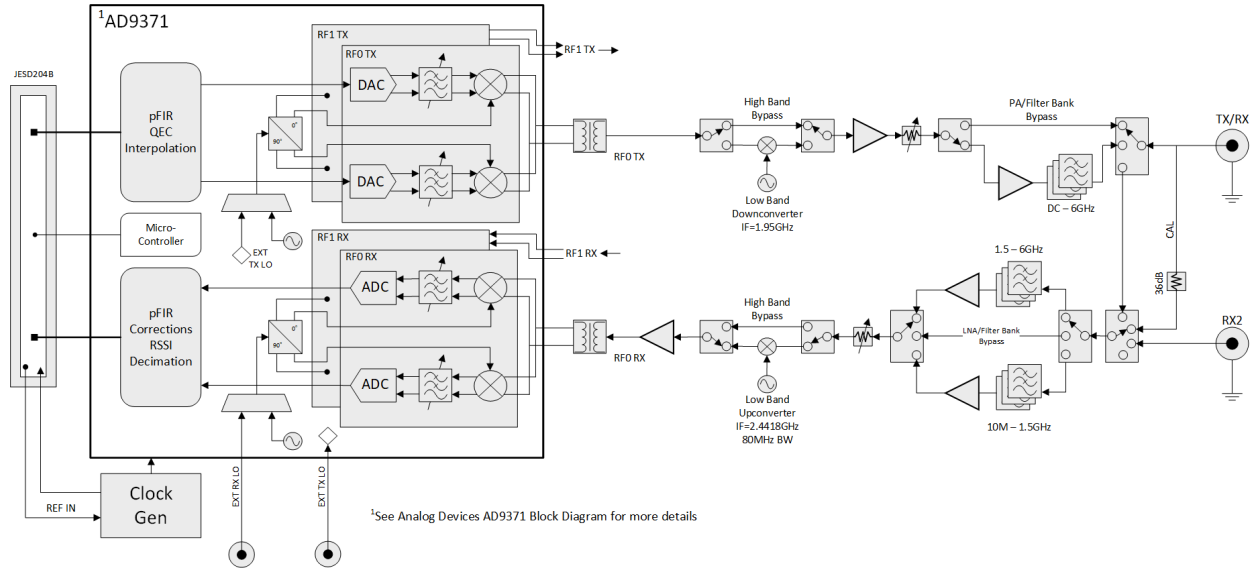


Figure 10: Ettus USRP N310 Transceiver (Tx/Rx)

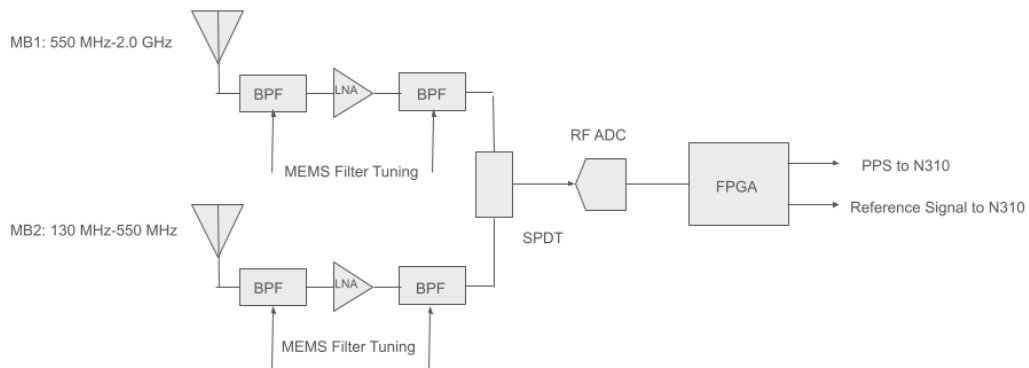


Figure 11: Pulsar Timing Design

Figures 12 and 13 show the components in a modern FPGA and a System-on-Chip (SoC) FPGA, respectively.

Components in a modern FPGA

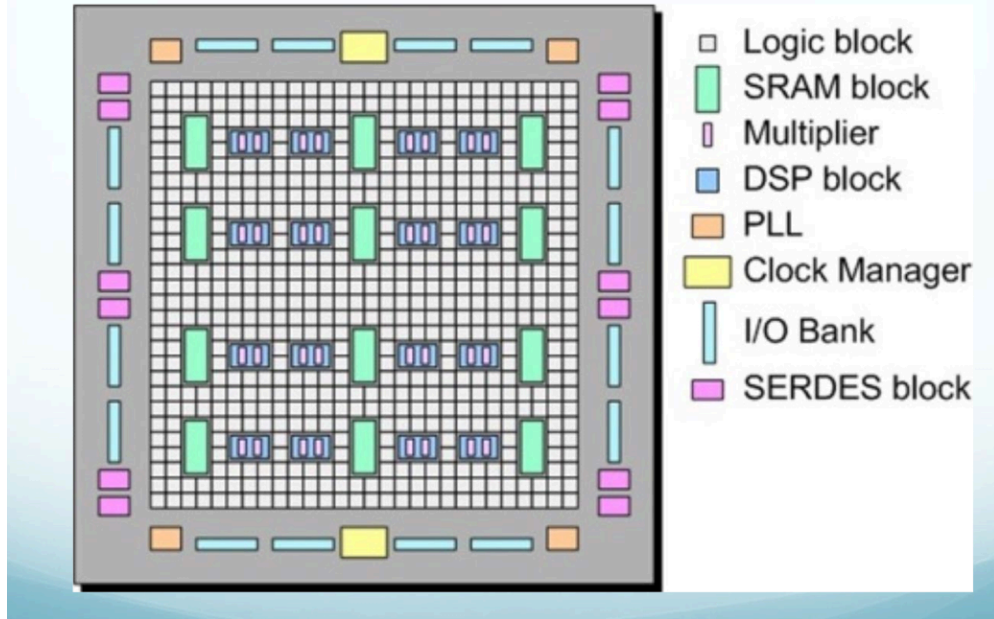


Figure 12: Components in a Modern FPGA

(Courtesy: Introduction to Field Programmable Gate Arrays, Hannes Sakulin CERN / EP-CMD)

System-On-a-Chip (SoC) FPGAs

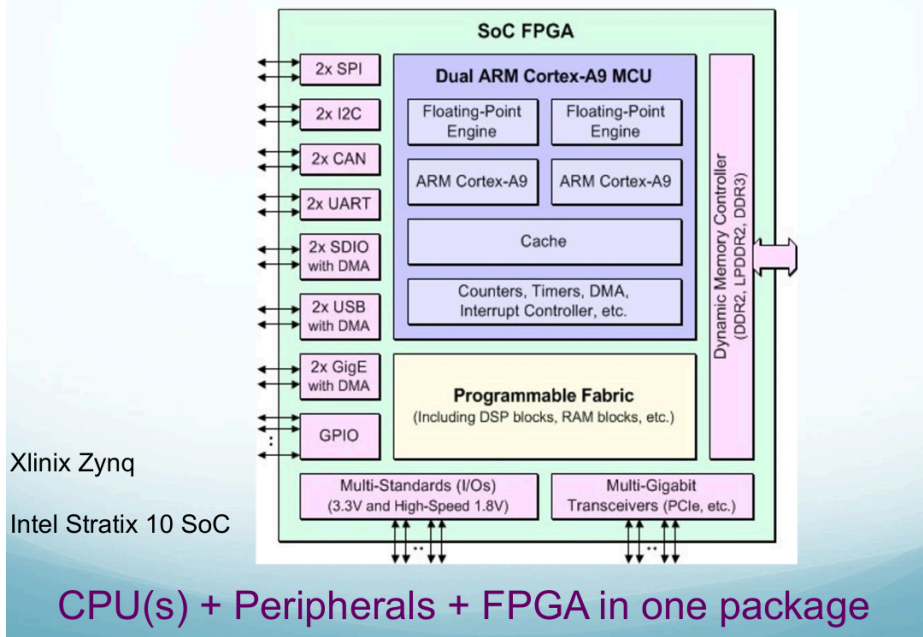


Figure 13: SoC FPGA

(Courtesy: Introduction to Field Programmable Gate Arrays, Hannes Sakulin CERN / EP-CMD)

5. CubeSat Communications

Figure 14 shows the CubeSat uplink/downlink system (Figure A11 from Hinzel, D., 2024, TechRxiv). This system must communicate with the ground station and all of the other CubeSats in the interferometer array. An ideal communications protocol is Code Division Multiple Access (CDMA). For space-based communication applications, CDMA has been used for many decades due to the large path loss and Doppler shift caused by satellite motion. CDMA is often used with [Binary Phase Shift Keying \(BPSK\)](#) in its simplest form, but can be combined with any modulation scheme like (in advanced cases) [Quadrature Amplitude Modulation \(QAM\)](#) or [Orthogonal Frequency Division Multiplexing \(OFDM\)](#), which typically makes it very robust and efficient (and equipping them with accurate ranging capabilities, which is difficult without CDMA). Other schemes use subcarriers based on [Binary Offset Carrier Modulation \(BOCM\)](#), which is inspired by [Manchester codes](#) and enable a larger gap between the virtual center frequency and the subcarriers, which is not the case for OFDM subcarriers.

The proposed CubeSat interferometer array architecture consists of three mutually orthogonal linear arrays, each supporting four CubeSat elements (Figure A7 from Hinzel, D., 2024, TechRxiv). The communications system must be able to access all twelve CubeSats as well as the ground station operating the network. Figure 15 illustrates a notional depiction of CDMA where $N=13$ (12 CubeSats plus the ground station). CDMA allows multiple transmitters to send information simultaneously over a single communication channel by employing spread spectrum technology and a special coding scheme. This method optimizes the use of available bandwidth as it transmits over the entire frequency range and does not limit the user's frequency range. Each of the twelve CubeSats and the ground station is assigned a unique code and the data transmission is combined so that each element in the network receives all of the information about all the other elements. The separation of signals is achieved by correlating the received signal with the locally generated code of the desired user. As shown in Figure 14, all of the CDMA signal processing can be handled by the FPGA, and possibly ASICs and other DSP assets.

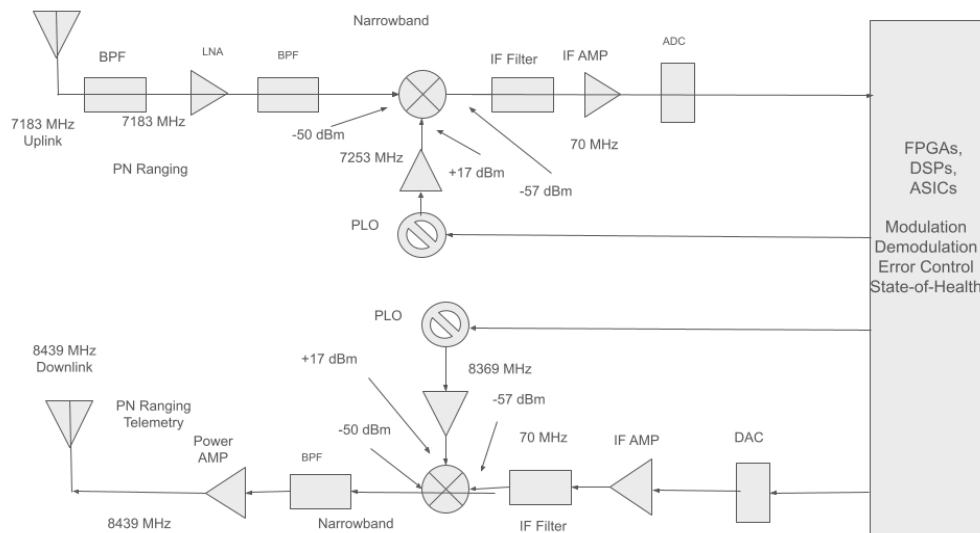


Figure 14: CubeSat Uplink/Downlink System

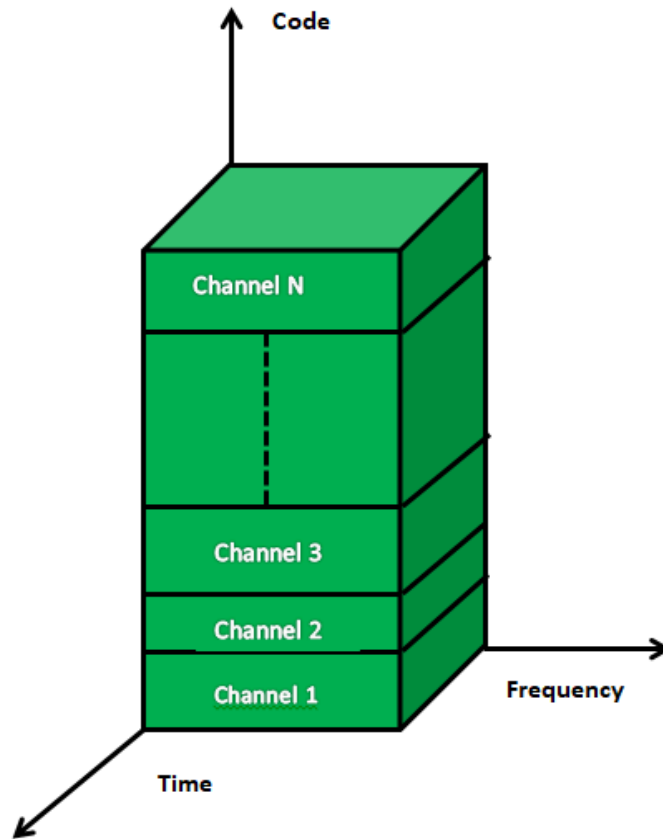


Figure 15: Code Division Multiple Access (CDMA) Structure

6. CubeSat System Demonstration

Figure 16 shows a notional concept for testing the pulsar timing design. Here, two RF signal generators transmit signals to the 4-element interferometer. One signal generator operates in a pulsed mode thereby simulating the pulsar timing signal. The other signal generator produces a signal which is the radio frequency counterpart of a given high energy astrophysical phenomena (e.g., Active Galactic Nebula). The outputs of the interferometer are displayed and measured on an oscilloscope (or alternately a spectrum analyzer). The performance of the individual receivers as well as the entire interferometer array can be determined.

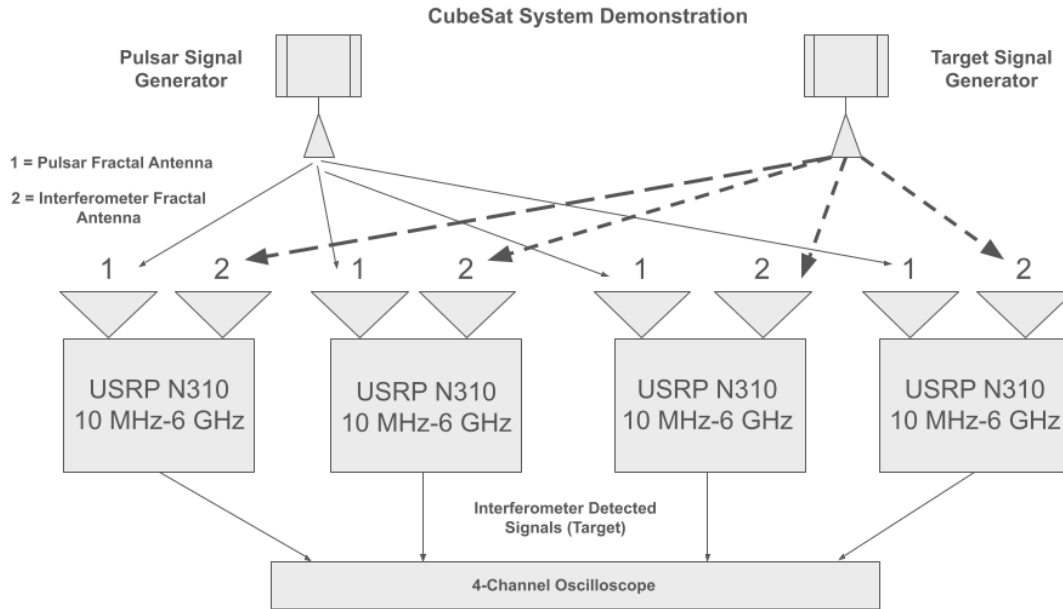


Figure 16: CubeSat System Demonstration

7. Conclusions

This study, in combination with Hinzel, D., 2024, TechRxiv, clearly illustrates that CubeSat very long baseline interferometer systems that incorporate pulsar timing beyond low earth orbit are a feasible approach to the detection of radio frequency counterparts of high energy astrophysical phenomena.

References

[“Application of CubeSats for Astrophysics Research: Detection of Radio Frequency Counterparts of High Energy Phenomena with Very Long Baseline Interferometry”](#), TechRxiv, DOI: [10.36227/tech-arxiv.172902594.41726347/v1](#), Hinzel, D., 2024, TechRxiv

[“LOFAR Discovery of a 23.5 s Radio Pulsar”](#) Tan, C. M., et al., 2018 *ApJ* 866 54, DOI [10.3847/1538-4357/aade88](#)

[“Photometric Observations of Nine High Mass X-Ray Binaries and Analysis of Potential Periodicities and Variations”](#) Hinzel, D., 2022 *Res. Notes AAS* 7 15; DOI [10.3847/2515-5172/acb5a0](#).

[“Recent Outbursts of the High-mass X-Ray Binary CI Camelopardalis”](#) Hinzel, D., 2024 *Res. Notes AAS* 8 124; DOI [10.3847/2515-5172/ad4646](#).

Wikipedia: Multiple References

[The ATNF Pulsar Catalogue](#)

Jodrell Bank Pulsar Group

National Radio Astronomy Observatory (NRAO)

PRESTO: Pulsar Exploration and Search TOOLkit

Appendix

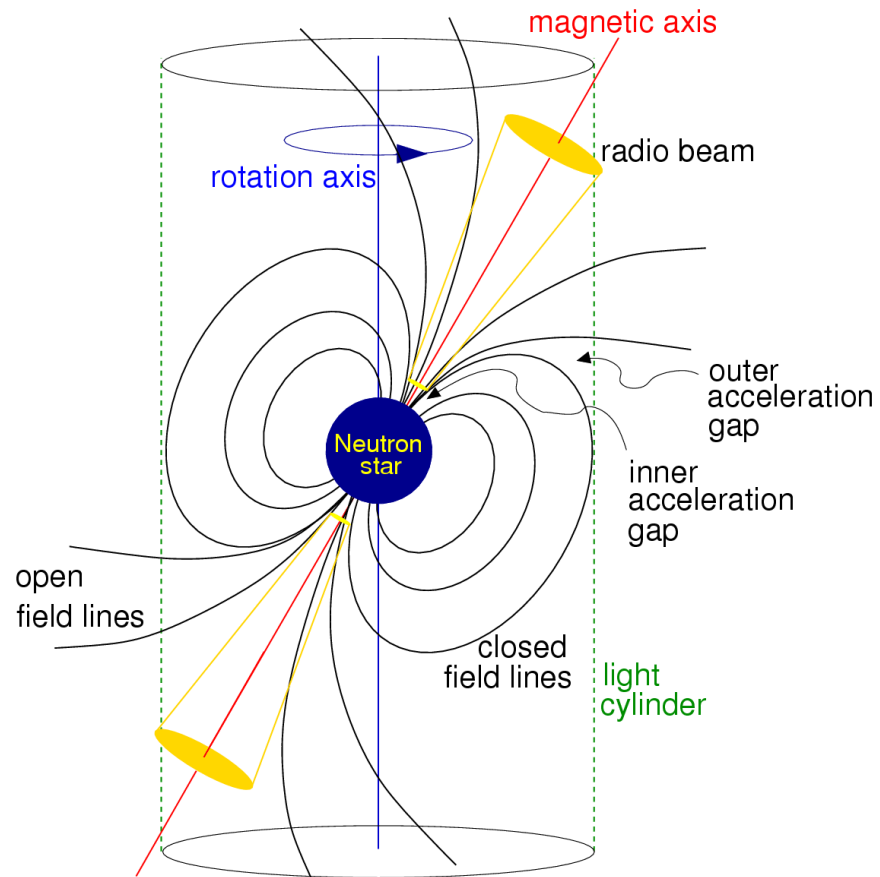


Figure A1: Pulsar Geometry

(Lorimer, D. and Kramer, M., Handbook of Pulsar Astronomy: Cambridge University Press, 2004)

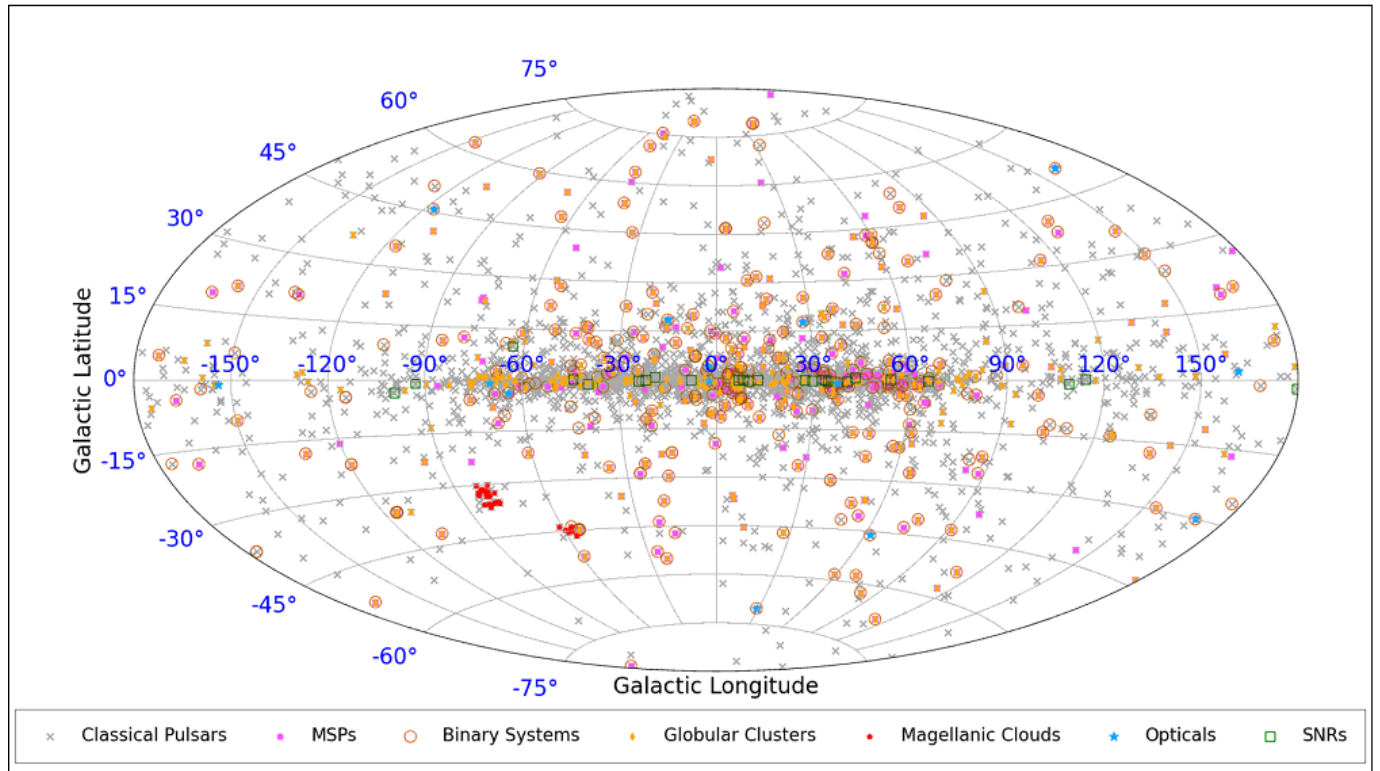
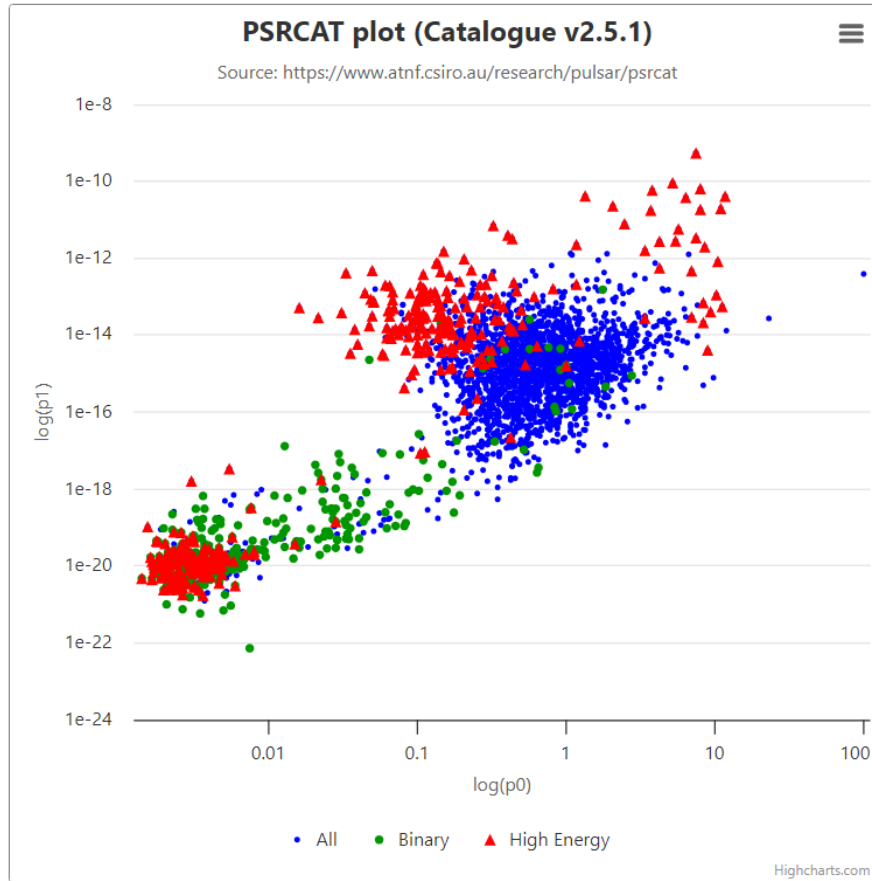


Figure A2: The Galactic Distribution of Milky Way Pulsars (Credit: Rami Mandow)

ATNF Pulsar Catalogue

Catalogue Version: 2.5.1



Toggle logarithmic x-axis

Toggle logarithmic y-axis

Figure A3: The ATNF Pulsar Catalog

Parameters utilized by [The ATNF Pulsar Catalogue](#) follow:

JNAME	J1935+1616
RAJ	19:35:47.857
DECJ	+16:16:40.60
PEPOCH	42264.5
P0	0.358736248270
P1	6.00354e-15
DM	158.53
RM	-1.9

PMRA	2
PMDEC	-25
POSEPOCH	40213
S400	242
S1400	42
W10	17.7
W50	9.0
F0	2.78756329984
F1	-4.66506e-14
AGE	1.0
BSURF	1.49
EDOT	5133.83
RAJD	293.9494
DECJD	16.2779
GI	52.44
Gb	-2.09
R_LUM	15218.15
R_LUM14	2641.17
DIST_DM	7.93
TAU_SC	1.51e-05
SURVEY	jb1,ar1,mol2,gb3,ar2,ar3
DM*sin(b)	-5.79
OSURVEY	0000002616
PMTOT	25
VTRANS	939.90
P1_I	5.99922
AGE_I	1.0
BSURF_I	1.48
EDOT_I	5130.13
EDOTD2	682.17
XX	6.28
YY	3.67
ZZ	-0.29
DIST	7.93

The Pulsar Parameters:

Name: Pulsar name. The B name if exists, otherwise the J name.
 JName: Pulsar name based on J2000 coordinates
 RAJ: Right ascension (J2000) (hh:mm:ss.s)
 DecJ: Declination (J2000) (+dd:mm:ss)
 PMRA: Proper motion in the right ascension direction (mas/yr)
 PMDec: Proper motion in declination (mas/yr)

PX: Annual parallax (mas)
PosEpoch: Epoch of position, defaults to PEpoch (MJD)
ELong: Ecliptic longitude (degrees)
ELat: Ecliptic latitude (degrees)
PMElong: Proper motion in the ecliptic longitude direction (mas/yr)
PMElat: Proper motion in ecliptic latitude (mas/yr)
GL: Galactic longitude (degrees)
GB: Galactic latitude (degrees)
RAJD: Right ascension (J2000) (degrees)
DecJD: Declination (J2000) (degrees)

Timing solution and profile parameters:

P0: Barycentric period of the pulsar (s)
P1: Time derivative of barycentric period (dimensionless)
F0: Barycentric rotation frequency (Hz)
F1: Time derivative of barycentric rotation frequency (s⁻²)
F2: Second time derivative of barycentric rotation frequency (s⁻³)
F3: Third time derivative of barycentric rotation frequency (s⁻⁴)
PEpoch: Epoch of period or frequency (MJD)
DM: Dispersion measure (cm⁻³ pc)
DM1: First time derivative of dispersion measure (cm⁻³ pc yr⁻¹)
RM: Rotation measure (rad m⁻²)
W50: Width of pulse at 50% of peak (ms). Note, pulse widths are a function of both observing frequency and observational time resolution, so quoted widths are indicative only. Refer to the original reference for details.
W10: Width of pulse at 10% (ms). Note the comments above for W50.
Units: Timescale for period/frequency and epoch data: TCB or TDB. See Hobbs, Edwards & Manchester (2006) for a discussion of the relationship between TCB and TDB.
Tau_sc: Temporal broadening of pulses at 1 GHz due to interstellar scattering (s).
Note: values measured at other frequencies are scaled assuming $\text{Tau_sc} \sim \nu^{-4.4}$.
S400: Mean flux density at 400 MHz (mJy)
S1400: Mean flux density at 1400 MHz (mJy)
S2000: Mean flux density at 2000 MHz (mJy)

Binary system parameters:

Binary: Binary model (usually one of several recognised by the pulsar timing programs TEMPO or TEMPO2).
Modified versions of standard models are often used - refer to the source paper for details of the binary model used.
T0: Epoch of periastron (MJD)
PB: Binary period of pulsar (days)
A1: Projected semi-major axis of orbit (lt s)

OM: Longitude of periastron (degrees)
ECC: Eccentricity
TASC: Epoch of ascending node(MJD) - ELL1 binary model
EPS1: $ECC \times \sin(OM)$ - ELL1 binary model
EPS2: $ECC \times \cos(OM)$ - ELL1 binary model
MinMass: Minimum companion mass assuming $i=90$ degrees and neutron star mass is 1.35 M_{\odot}
MedMass: Median companion mass assuming $i=60$ degrees
BinComp: Companion type

Distance parameters:

Dist: Best estimate of the pulsar distance using the YMW16 DM-based distance as default (kpc)
Dist_DM: Distance based on the YMW16 electron density model.
In 'LONG' or 'PUBLICATION QUALITY' modes, lower limits from the distance model are preceded by a '+' sign.
DMsinb: $DM \times \sin(b)$ ($\text{cm}^{-3} \text{ pc}$)
ZZ: Distance from the Galactic plane, based on Dist
XX: X-Distance in X-Y-Z Galactic coordinate system (kpc)
YY: Y-Distance in X-Y-Z Galactic coordinate system (kpc)

Associations and survey parameters:

Assoc: Names of other objects, e.g., supernova remnant, globular cluster or gamma-ray source associated with the pulsar
Survey: Surveys that detected the pulsar (discovery survey first). [Click here for currently defined surveys.](#)
OSurvey: Surveys that detected the pulsar encoded as bits in integer
Date: Date of discovery publication.
Type: Type codes for the pulsar. [Click here for available types.](#)
NGlt: Number of glitches observed for the pulsar

Derived parameters:

R_Lum: Radio luminosity at 400 MHz (mJy kpc^2)
R_Lum14: Radio luminosity at 1400 MHz (mJy kpc^2)
Age: Spin down age (yr) []
BSurf: Surface magnetic flux density (Gauss) []
Edot: Spin down energy loss rate (ergs/s)
Edotd2: Energy flux at the Sun ($\text{ergs/kpc}^2/\text{s}$)
PMTot: Total proper motion (mas/yr)
VTrans: Transverse velocity - based on DIST (km/s)
P1_i: Period derivative corrected for Shklovskii (proper motion) effect
Age_i: Spin down age from P1_i (yr)
BSurf_i: Surface magnetic dipole from P1_i (gauss)
B_LC: Magnetic field at light cylinder